Highlights on Spanish Astrophysics IX, Proceedings of the XII Scientific Meeting of the Spanish Astronomical Society held on July 18 – 22, 2016, in Bilbao, Spain. S. Arribas, A. Alonso-Herrero, F. Figueras, C. Hernández-Monteagudo, A. Sánchez-Lavega, S. Pérez-Hoyos (eds.)

Revealing the location of the mixing layer in a hot bubble

M.A. Guerrero[1], X. Fang[1,2], Y.-H. Chu[3] J.A. Toalá[1,3] and R.A. Gruendl[4]

[1]Instituto de Astrofísica de Andalucía (IAA-CSIC), Glorieta de la Astronomía s/n, E-18008 Granada, Spain
[2]Department of Physics, The University of Hong Kong, Pokfulam Road, Hong Kong
[3]Institute of Astronomy and Astrophysics, Academia Sinica (ASIAA), Taipei 10617, Taiwan
[4]Department of Astronomy, University of Illinois, 1002 West Green Street, Urbana, IL 61801, USA

Abstract

The fast stellar winds can blow bubbles in the circumstellar material ejected from previous phases of stellar evolution. These are found at different scales, from planetary nebulae (PNe) around stars evolving to the white dwarf stage, to Wolf-Rayet (WR) bubbles and up to large-scale bubbles around massive star clusters. In all cases, the fast stellar wind is shock-heated and a hot bubble is produced. At the mixing layer between the hot bubble and optical nebula, processes of mass evaporation and mixing of nebular material and heat conduction are key to determine the thermal structure of these bubbles and their evolution. In this contribution we review our current understanding of the X-ray observations of hot bubbles in PNe and present the first spatially-resolved study of a mixing layer in a PN.

1 Introduction

Planetary nebulae (PNe) are the progeny of low- and intermediate-mass stars with initial masses $\leq$810 $M_{\odot}$. As these stars ascend the asymptotic giant branch (AGB), they experience episodes of heavy mass loss through a slow (v_{∞} $\sim$10 km s^1) wind. Once the stellar envelope is lost and the stellar core is exposed, the stellar wind increases its terminal velocity up to 1000-4000 km s^1 [3, 11]. This fast wind sweeps up the slow AGB wind, which is further photoionized by the central star (CSPN) to form a PN [17, 6].

The interaction between these two stellar winds produces hot gas that fills a hot bubble in the inner region of the PN. Extended X-ray emission has now been detected inside the inner cavities of nearly 30 PNe with plasma temperatures of (13)$\times$10^6 K and electron densities

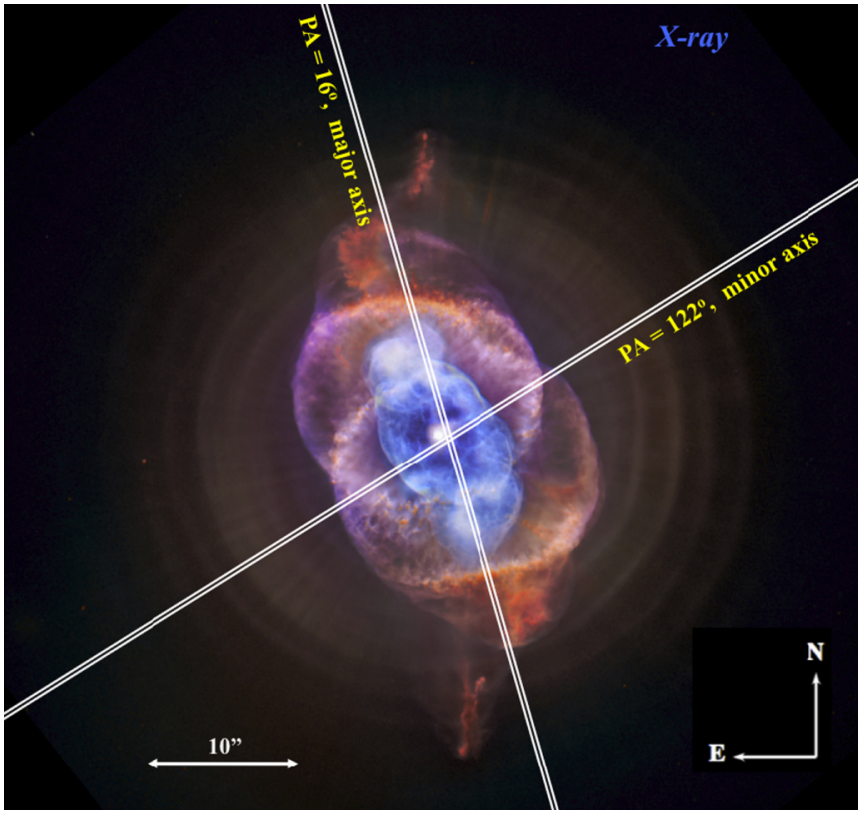

Figure 1: *HST* optical (red, purple) and *Chandra* X-ray (blue) color-composite image of NGC 6543. Image adopted from the *Chandra* X-ray Center (http://chandra.harvard.edu/photo/2008/catseye/). The positions of the *HST* STIS $52'' \times 0.2''$ long slit are marked with white lines.

of 110 cm^3 (e.g. [9, 12, 10, 15, 16, 13, 14, 4, 7]). The *"low"* temperature and *"high"* density of the X-ray-emitting plasma in PNe, as compared to those predicted in simple models of adiabatically shocked stellar winds, suggests that some mechanism is reducing the temperature of the hot bubble and raising its density. Thermal conduction ([20, 21] and references therein) and/or hydrodynamical instabilities (e.g. [22, 23]) in the windwind interaction zone can inject material into the hot bubble, creating a mixing layer of gas with intermediate temperatures ($\sim$10^5 K) between the hot bubble and the optical nebular shell.

X-ray observations of NGC 6543 (a.k.a. the Cat's Eye Nebula) reveal a physical structure qualitatively consistent with the ISW models (Chu et al. 2001). The *Chandra* image of NGC 6543 (Fig. 1) shows simple limb-brightened diffuse X-ray emission confined within the bright inner shell and two blisters at the tips of its major axis, in sharp contrast to its complex optical morphology [1]. The observed X-ray temperature (1.7×10^6 K; [4]) is much lower than that expected for a stellar wind of v_∞ $\sim$1400 km s^1 [18]. The morphology and physical conditions of the hot plasma are suggestive of the presence of a mixing layer in NGC 6543.

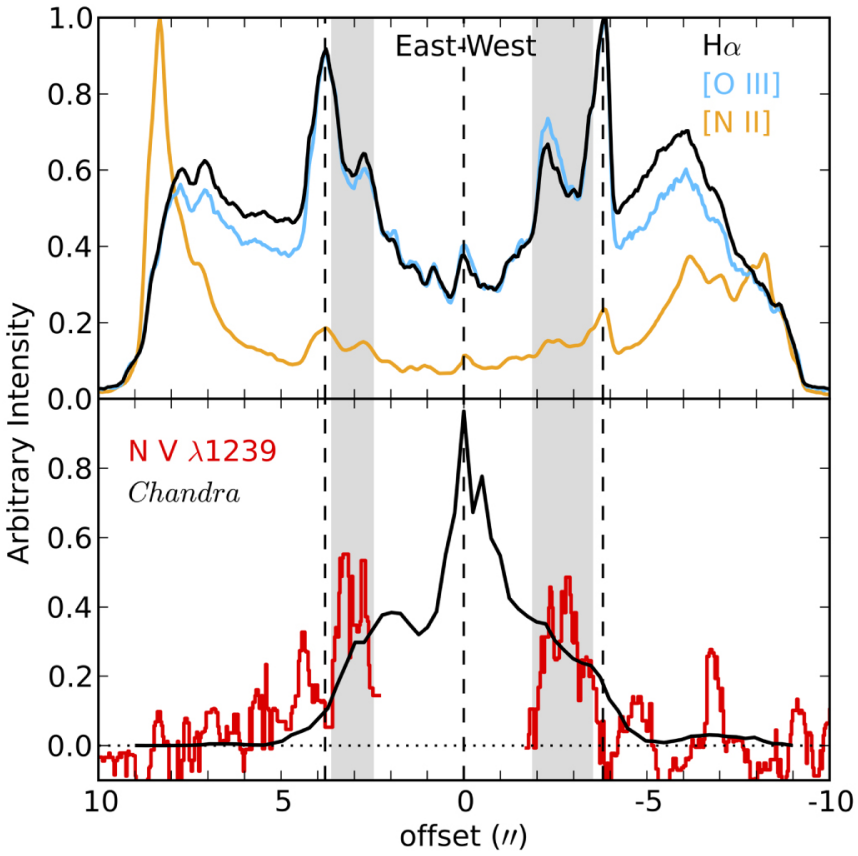

Figure 2: Spatial emission profiles of the Hα, [O III] λ5007, and [N II] λ6583 emission lines from the optical nebular shell (top panel), and the N V λ1239 UV resonance line from the interface layer and the *Chandra* X-ray emission from the hot bubble (bottom panel) along the minor axis of NGC 6543 at PA 122° (Fig. 1). The offset is relative to the CSPN. Gray shaded areas mark the positions of the interface layer, as indicated by the N V line.

2 Observations and Data Analysis

HST STIS UV and optical spectroscopic observations of NGC 6543 (PI: M.A. Guerrero, GO prop. ID 12509, Cycle 19) were carried out on 2012 July 3 and October 21. The observations aimed to detect and trace the spatial extent of the interface layer and compare it with the layers of the nebular shell and hot bubble. The $52'' \times 0.2''$ long slit was placed at position angles (PAs) of 16° and 122° along the major and minor axes of the inner nebular shell (Fig. 1), respectively. The G140M grating and STIS/FUV-MAMA detector were used to acquire spectra of the N V $\lambda\lambda$1239,1243 and C IV $\lambda\lambda$1548,1551 emission lines. The G430L and G750M gratings and STIS/CCD detector were used to obtain information on the [O III], Hα, and [N II] lines from the optical nebular shell.

The two-dimensional (2D) STIS spectra were used to extract spatial profiles of emission along the minor axis of the photoionized innermost nebular shell for the Hα, [O III] λ5007,

and [N II] λ6583 lines (Fig. 2, top panel) and the collisionally excited N V λ1239 UV line (Fig. 2, bottom panel). The spatial profile of the X-ray emission, as derived from the *Chandra* observations, is added into the bottom panel of Fig. 2.

3 Results and Discussion

The spatial profiles along the minor axis of NGC 6543 (Fig. 2) reveal the location of mixing layer gas originating from very different processes. The brightest emission peaks in Hα and [O III] at $\sim 4''$ from the CSPN mark the location of the $\sim 10^4$ K swept-up inner nebular shell. On the other hand, the profile of the X-ray emission from the $\geq 10^6$ K hot gas shows an eastern peak at $\sim 2''$ and a shoulder of declining emission toward the west. This irregular profile suggests that the X-ray-emitting gas is confined within a region with radius $\leq 3''$. Therefore, the X-ray-emitting gas is confined within the cool nebular shell.

Interestingly, the spatial profile of the N V emission peaks at intermediate positions (gray shades in Fig. 2), between the optical lines from the optical nebular shell and the X-ray emission from the hot bubble. We remind that the N V ion cannot be produced by photoionization because the effective temperature of the CSPN of NGC 6543 is 50,000 K; thus it must be produced by thermal collisions at temperatures of $\sim 10^5$ K, as expected in the mixing layer.

The spatial profile of the N V λ1239 emission line has been used to estimate an outer radius and thickness of the mixing layer of $\sim 3.7''$ and $1.0''$, respectively. At a distance of 1.0 ± 0.3 kpc [19], this implies a thickness of 1.5×10^{16} cm.

The density of the mixing layer can also be estimated to be ~ 180 cm^{-3}, assuming a simple geometry for the N V λ1239-emitting region and a $N^{4+}/H+$ ionic abundance ratio close to the nebular nitrogen abundance (N/H) of 2.3×10^4 [2]. This density and the adopted temperature of 2×10^5 K imply a thermal pressure of 2×10^8 dyn cm^2 in the mixing layer, which agrees with the pressure of the hot bubble and the ionized swept-up shell [8].

To sum up, we have presented high-spatial resolution *HST* STIS UV and optical spectroscopy of the Cat's Eye Nebula (NGC 6543). These STIS observations have enabled the first view of the spatial distribution of the mixing layer gas, as probed by the collisionally ionized N V UV emission line. The mixing layer is located exactly between the optical nebular rim and the X-ray-emitting hot bubble as previously detected by *Chandra*. The hot gas in the mixing layer is in hydrodynamical equilibrium with the hot bubble and ionized nebular rim. More extended details of this work are reported by [5].

Acknowledgments

Support for the Hubble Space Telescope Cycle 20 General Observer Program 12509 was provided by NASA through grant HST-GO-12509.01-A from the Space Telescope Science Institute, which is operated by the Association of Universities for Research in Astronomy, Inc., under NASA contract NAS 5-26555. X.F., M.A.G., and J.A.T. are partially funded by grants AYA 2011-29754-C03-02 and AYA 2014-57280-P of the Spanish MEC (Ministerio de Economía y Competitividad), cofunded with

FEDER funds.

References

[1] Balick B. 2004, AJ, 127, 2262

[2] Bernard-Salas J., Pottasch S.R., Wesselius P.R., Feibelman W.A. 2003, A&A, 406, 165

[3] Cerruti-Sola M., Perinotto M. 1985, ApJ, 291, 237

[4] Chu Y.-H., Guerrero M.A., Gruendl R.A. et al. 2001, ApJL, 553, L69

[5] Fang, X., Guerrero, M. A., Toalá, J. A., Chu, Y.-H., & Gruendl, R. A. 2016, ApJL, 822, L19

[6] Frank A., Balick B., Riley J. 1990, AJ, 100, 1903

[7] Freeman M., Montez R.Jr., Kastner J.H. et al. 2014, ApJ, 794, 99

[8] Gruendl R.A., Chu Y.-H., Guerrero M.A., 2004, ApJL, 617, L127

[9] Guerrero M.A., Chu Y.-H., Gruendl R.A. 2000, ApJS, 129, 295

[10] Guerrero M.A., Chu Y.-H., Gruendl R.A., Meixner M. 2005, A&A, 430, L69

[11] Guerrero M.A., de Marco O. 2013, A&A, 553, A126

[12] Guerrero M.A., Gruendl R.A., Chu Y.-H. 2002, A&A, 387, L1

[13] Kastner J.H., Montez R. Jr, Balick B. and De Marco O. 2008 ApJ 672 957

[14] Kastner J.H., Montez R.Jr, Balick B. et al. 2012, AJ, 144, 58

[15] Kastner J.H., Soker N., Vrtilek S.D., Dgani R. 2000, ApJL, 545, L57

[16] Kastner J.H., Vrtilek S.D., Soker N. 2001, ApJ, 550, 189

[17] Kwok S. 1983 Proc. IAU Symp. 103, Planetary Nebulae ed D.R. Flower, 293 (Dordrecht: D. Reidel)

[18] Prinja R.K., Hodges S.E., Massa D.L., Fullerton A.W., Burnley A.W. 2007, MNRAS, 382, 299

[19] Reed D.S., Balick B., Hajian A.R. et al. 1999, AJ, 118, 2430

[20] Soker N. 1994, AJ, 107, 276

[21] Steffen M., Schönberner D., Warmuth A. 2008, A&A, 489, 173

[22] Toalá J.A., Arthur S.J. 2014, MNRAS, 443, 3486

[23] Toalá J.A., Arthur S.J. 2016, MNRAS, 463, 4438